A Quantum Mechanical/Molecular Mechanical Model of Inhibition of the Enzyme Phospholipase A_2

Bohdan Waszkowycz,†[a] Ian H. Hillier,*[a] Nigel Gensmantel[b] and David W. Payling[b]
[a] *Department of Chemistry, University of Manchester, Manchester M13 9PL, UK*
[b] *Fisons plc, Pharmaceuticals Division, Bakewell Road, Loughborough, Leicestershire LE11 0RH, UK*

The mechanism of catalysis within the enzyme phospholipase A_2 has been investigated by a combination of *ab initio* molecular orbital, molecular mechanics and free energy perturbation calculations. The computational model has been used to quantify the energetics of binding and hydrolysis of a carbamate phospholipid, and to rationalise the differences in reactivity of carbamate, ester and amide phospholipids. The binding of fluorinated ketone analogues is also discussed. A number of aspects of the calculations are critically examined and the method is shown to be a powerful tool in the investigation of catalytic reaction paths in macromolecular systems.

In our earlier papers, we discussed the potential of an integrated molecular mechanical/quantum mechanical approach to the investigation of the mechanism of catalysis of the enzyme phospholipase A_2 (PLA2).[1–3] Here we present a further application of this methodology, in order to describe in some detail the energetics of binding and hydrolysis of a number of inhibitors of PLA2.

Previously the computational model was applied to the mechanism of hydrolysis of ester and amide phospholipids, which are, respectively, a substrate and an inhibitor of the enzyme.[2] In the present paper we contrast their behaviour with that of a further inhibitor, a phospholipid analogue in which the ester linkage is replaced by a carbamate linkage. We also discuss the binding of phospholipid analogues in which the ester is replaced by a fluorinated ketone moiety. These examples are presented in order to demonstrate the value and the limitations of a purely theoretical approach to the modelling of the energetics of substrate binding and hydrolysis.

PLA2 has a fundamental role in cell regulation, being responsible for the hydrolysis of the phospholipids of cell membranes to release fatty acids such as arachidonic acid.[4] This is the initial step in the production of a diverse range of cellular mediators such as the prostaglandins. Inhibition of PLA2 is a potentially important route to the treatment of various inflammatory disorders, and therefore an understanding of the mechanism of catalysis may contribute to rational drug design.[5]

The basis for our calculations has been a mechanism of catalysis originally proposed by Verheij *et al.*[6] from limited experimental data. This mechanism has recently been supported by the first published X-ray structures of PLA2 compelxed with an amide inhibitor and a transition state analogue.[7] As experimental evidence for the details of the mechanism remain scarce, the application of theoretical calculations offers a potentially powerful route by which to explore aspects of catalysis which are less amenable to experiment.

In brief, the computational method involved the initial modelling of the macromolecular structures of enzyme–substrate complexes with the use of molecular mechanics and dynamics in the program AMBER,[8] in order to determine the mode of substrate binding in the absence of crystallographic evidence. These refined structures were the basis for *ab initio* molecular orbital calculations on the important active-site residues within the program GAMESS,[9] from which an estimate of the barrier to substrate hydrolysis was obtained. The free energies of binding of the phospholipid analogues to PLA2 were evaluated by means of free-energy perturbation methods, as implemented in the GIBBS module of AMBER.

The combination of empirical and quantum mechanical techniques is becoming a powerful tool in the investigation of enzyme catalysis. Molecular mechanics (MM) can readily be applied to macromolecular systems as an efficient means of exploring the structures and conformational energies of enzyme–substrate complexes.[10] However, molecular orbital (MO) methods remain necessary for the description of electronic properties, most importantly for the evaluation of the energetics of bond formation or dissociation.

Our concern has been to develop an MO model which is able to provide a realistic description of the energetics of catalysis within the environment of the enzyme active-site. For the foreseeable future, computational expense will severely limit the size of supermolecule system which can be treated at a meaningful level of MO theory. As a result, any supermolecule model will represent only a few fragments of the substrate and the active-site residues, and will neglect the steric and electrostatic interactions provided by the bulk environment. It is therefore appropriate to attempt to integrate an MO approach with MM methods in order to provide a more complete picture of the bulk system.

At the simplest level, the MO calculation describes a small number of quantum mechanical (QM) atoms which represent, for example, the residues of the enzyme active site, in order to evaluate the energetics of the catalytic potential energy surface.[11] MM may be used to model the structure of the macromolecular system and estimate the energy of interaction of the bulk enzyme with the QM supermolecule.[12] The electrostatic component of this interaction may also be efficiently modelled by placing the QM supermolecule within a field of partial point charges, which explicitly represent the atoms of the bulk environment. In this way it is possible to reproduce the polarisation of the catalytic residues by the bulk enzyme, which is often an important factor in the activation of reactants or the stabilisation of intermediates.[13]

More formal integrations of MO and MM methods have also been developed, in which the MM forces exerted by the environment are allowed to influence the course of a geometry optimisation of the QM system.[14,15] Therefore it becomes possible to investigate the influence of the active site on the geometry of reactive intermediates, rather than rely on the more

† *Present address:* Proteus Molecular Design Ltd, 48 Stockport Road, Marple, Cheshire SK6 6AB.

usual assumption that an *in vacuo* geometry is adopted. The method which has been used here is a development of the program QUEST of Singh and Kollman.[14]

The above techniques have been applied in the current paper to an investigation of the energetics of hydrolysis of a carbamate phospholipid. MM has been used to model the binding of the phospholipid to the active site of PLA2, as well as that of the oxyanion presumed to be an intermediate in its hydrolysis. Qualitative differences between the mode of binding of the carbamate with that of ester and amide phospholipids have been examined, and in particular the influence of substrate conformation.

MO calculations have been performed on supermolecule systems which represent the most important active site residues, in order to evaluate the QM energy of the oxyanion intermediate relative to that of the carbamate reactant. In this way, a measure of the barrier to substrate hydrolysis is obtained, which may be used to compare quantitatively the ease of hydrolysis of different substrates, and to assess the contribution to catalysis of various active-site residues. These calculations were performed with the incorporation of a field of point charges in the one-electron Hamiltonian to produce the electrostatic potential of the bulk environment of the protein. The structures of the carbamate and oxyanion were first refined by means of the hybrid QM–MM optimisation, in order to gain some insight into the geometries of these species *in situ*, *i.e.* within the enzyme active site. The basis-set dependency of the calculations was investigated by means of calculations on smaller model systems at a range of basis sets and with the inclusion of electron correlation.

Complementary to the calculation of the barrier to hydrolysis is the calculation of the binding energy of the substrate to the active site. The free energy perturbation (FEP) method has recently received much attention as a feasible method for the calculation of solvation energies and enzyme–substrate binding energies which are in good agreement with experimental values.[16] The method allows a description of thermodynamic properties which has several advantages over the use of MM in the calculation of interaction energies. The statistical dynamics methodology enables the estimation of changes in entropy,[17] so that the calculated energies are Gibbs free energies rather than enthalpies, and may be thus related directly to experimental thermodynamic data. The implementation of a molecular dynamics simulation of the system allows the estimation of average energies of interaction between molecules, by consideration of a sample of the accessible conformational energy surface at a defined temperature and over a defined time-scale.[18] This overcomes the limitation of the MM method, which must rely on the evaluation of interaction energies at a single, minimum-energy, conformation, and which ignores the contribution of kinetic energy terms.

The FEP method is used here to investigate the free energies of binding of various phospholipid analogues to PLA2, and in particular to compare the binding of ester, amide and carbamate phospholipids. The papers of Gelb *et al.*[19] have prompted us to apply the technique to some fluorinated analogues. Certain fluorinated ketone analogues were reported to be potent inhibitors of PLA2, and it was presumed that the hydrated form of the ketone was likely to be the active inhibitor. In the absence of conclusive evidence, a theoretical evaluation of the binding energies of a fluorinated ketone and its hydrate was considered useful.

The proposed mechanism of catalysis can be summarised briefly. PLA2 specifically hydrolyses the 2-acyl ester bond of 1,2-diacyl-*sn*-3-glycerophosphatides (L-α-phospholipids, e.g. **1**). The recent X-ray structures of PLA2-inhibitor complexes[7] have confirmed that the phospholipid binds to the active-site calcium ion *via* the C^2 carbonyl and a phosphoryl oxygen, with

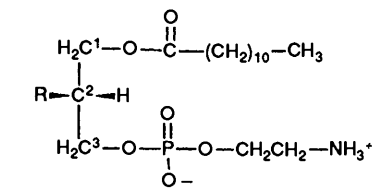

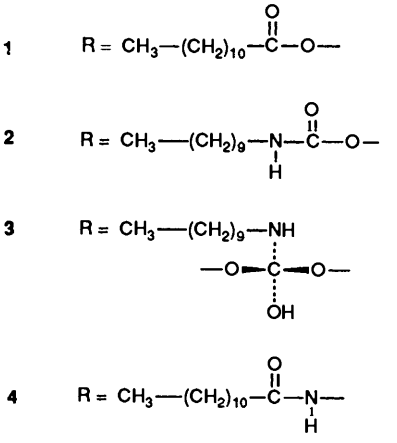

a hydrophobic interaction between the C^2 alkyl chain and the wall of the active site. This serves to position the C^2 carbonyl adjacent to a histidine–aspartate couple (His-48 and Asp-99 of bovine pancreatic PLA2), which is proposed to function similarly to the Ser–His–Asp triad of the serine proteases. In the case of PLA2, the nucleophile which attacks the C^2 carbonyl is presumed to be a water molecule, which is seen to be hydrogen-bonded to His-48 in the X-ray structure of the uncomplexed enzyme. Attack of this water molecule on the ester carbonyl would be concerted with proton transfer to the imidazole ring of His-48 (Fig. 1). The high-energy oxyanion intermediate which is formed is stabilised by the electrostatic interaction with the calcium ion and the ionic His–Asp couple. Proton transfer from His-48 to the C^2 ether oxygen leads to the breakdown of the oxyanion, and the release of the C^2 fatty acid.

Our earlier papers have investigated various aspects of this mechanism, and have confirmed that it is valid on structural and energetic grounds. Here we take the opportunity to apply the same computational model to the description of inhibition of the enzyme.

Computational Method

MM Modelling of PLA2–Inhibitor Complexes.—Models of the PLA2–phospholipid complexes for MM minimisation within AMBER were based on the crystal structure of bovine pancreatic PLA.[20] A carbamate inhibitor **2** was modelled, which is an analogue of the ester substrate considered in the earlier papers (1,2-dilauryl-3-*sn*-phosphatidylethanolamine, **1**), along with the oxyanion **3** which is presumed to be the intermediate formed on hydrolysis of **2**. As in the earlier work, the oxyanion is assumed to be similar to the true transition states in energy and in structure, and therefore the difference in quantum mechanical energy between the oxyanion and the reactant is taken as a measure of the barrier to substrate hydrolysis. (We have recently modelled the full potential energy surface in more detail, and have shown that this is a valid assumption.)[3] An amide analogue of the phospholipid **4** was also considered.

The complete enzyme (123 amino acid residues) was treated in the MM calculation. To the 106 water molecules in the crystal structure were added a further 640 within AMBER in order to achieve a complete solvation shell around the enzyme. A united-

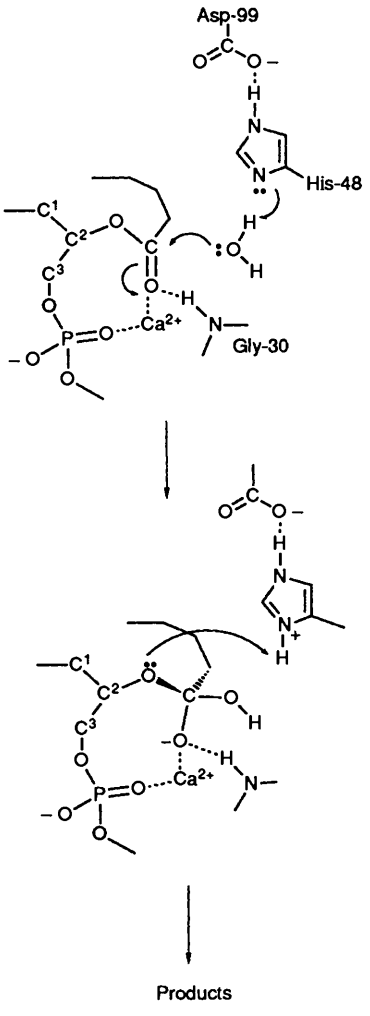

Fig. 1 The proposed mechanism of ester hydrolysis by PLA2

atom representation[21] was used for the bulk of the enzyme, with an all-atom representation[22] for the substrate and some 16 residues within the active site. In all, the solvated PLA2–substrate model comprised approximately 3500 atoms.

MM force-field parameters for the oxyanion intermediate were chosen to reproduce the structure of small model oxyanions as determined by *ab initio* geometry optimisation within GAMESS[9] at the level of a 3-21G basis set. Partial charges for the substrate were derived by the electrostatic potential (ESP) method of Singh and Kollman,[23] using an STO-3G basis set.

The conformation of the carbamate substrate was initially modelled on the X-ray structure of Hitchcock *et al.*,[24] in which the alkyl chains are in the extended and parallel conformation which is characteristic of a phospholipid within the lipid membrane (*i.e.* the same conformation as adopted for ester and amide substrates). As these calculations were performed before the X-ray structure of a PLA2–phospholipid complex became available, the substrate was positioned in the active site in accordance with the mechanism of Verheij *et al.*[6] The C^2 carbonyl and a phosphoryl oxygen were assumed to be bound to the calcium ion, with the C^2 alkyl chain adjacent to the hydrophobic wall of the active site.

The crystal structure of Thunnissen *et al.*[7] has demonstrated that an amide inhibitor is capable of binding in this manner. However, this structure differs from the Verheij mechanism in that the phospholipid is also hydrogen-bonded to His-48 (*via* the amide-NH), and thereby displaces the nucleophilic water (which is present in the uncomplexed enzyme). However, this does not rule out the role of water molecule as the nucleophile, since for an ester (or carbamate) substrate, an equivalent hydrogen bond to His-48 is not available.

The PLA2–carbamate complex was refined by standard steepest descent and conjugate gradient methods to convergence (*i.e.* a root-mean-square gradient below 0.1 kcal mol^{-1} $Å^{-1}$),* using a dielectric of 1 and a non-bonded cut-off of 8 Å. As mentioned above, the starting conformation of the carbamate substrate was modelled on that adopted by the ester phospholipid. In this conformation there is a kink in the C^2 chain, by which the C^2 and C^1 chains become parallel. Reproduction of this kink in the carbamate necessitates distortion of the amide linkage significantly away from planarity (Fig. 2). This was the conformation which was initially modelled (labelled as CAR1). As will be discussed later, the loss of planarity has a significant effect on the stability of the carbamate linkage and the ease of hydrolysis of the carbamate.

The minimisation of the carbamate was repeated in an attempt to maintain the planarity of the amide linkage. This was achieved with the use of computer graphics to model a suitable planar structure of the carbamate with which to begin the minimisation (*i.e.* with dihedrals of 180° for O^{21}–C^{21}–N^{22}–H^N and O^2–C^{21}–N^{22}–C^{23}; for atom labels, see Fig. 3). Initially, weak force constants were employed to impose planarity on the carbamate and to maintain a suitable carbonyl–calcium distance, but in the final minimisation all constraints were removed. This resulted in a conformation (CAR2) with the amide linkage near planarity, although still distorted somewhat from the ideally planar sp^2 nitrogen. This was caused by a less favourable steric interaction between the C^2 chain and the hydrophobic wall of the active site (note that the planarity of the amide linkage effectively increases the width of the C^2–C^{23} fragment), which also hindered the binding of the C^2 carbonyl to the calcium.

A final model of the carbamate reactant was generated by the use of molecular dynamics (MD), in order to assess other possible modes of binding. To reduce computational expense, the carbamate phospholipid and 46 amino acid residues around the active site were allowed to be mobile during MD, while all other residues were held fixed. Five water molecules were retained from the original PLA2–carbamate model (*i.e.* water molecules hydrogen-bonded within the active site), and the active site was then solvated with a spherical cap of 85 water molecules. After an initial minimisation of the water molecules to improve the water structure, MD was used to heat the system slowly to 300 K and the simulation was then continued for 4000 × 2 fs steps, before a final MM minimisation of the system with all constraints removed.

In this final structure (CAR3), the carbamate carbonyl is tightly bound to the calcium and the carbamate linkage remains approximately planar. The steric hindrance between the C^2 chain and the wall of the active site is relieved by a small translation of the carbamate away from the wall of the active site. The carbonyl achieves close binding to the calcium ion, but now loses the hydrogen bond to the -NH of Gly-30. Otherwise, the position of the alkyl chains and the phosphate group is very similar to previous models.

The oxyanion intermediate was modelled as in the earlier papers.[2] In order to achieve facile proton transfer from O^H to O^2 *via* His-48, it is necessary to assume that a doubly hydrogen-bonded conformation is adopted, in which the protonated His-48 is hydrogen-bonded to both oxygens (Fig. 4); this is similar to the intermediate proposed for the serine proteases,[25] and has recently been supported by the X-ray structure of PLA2 complexed with a transition state analogue.[7] Although such a conformation is achieved readily by a small oxyanion, it is

* 1 cal = 4.184 J.

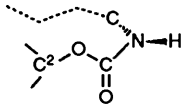

Fig. 2 Schematic representation of part of the carbamate in conformation CAR1, in which the torsion at the nitrogen results in the loss of planarity over the amide linkage

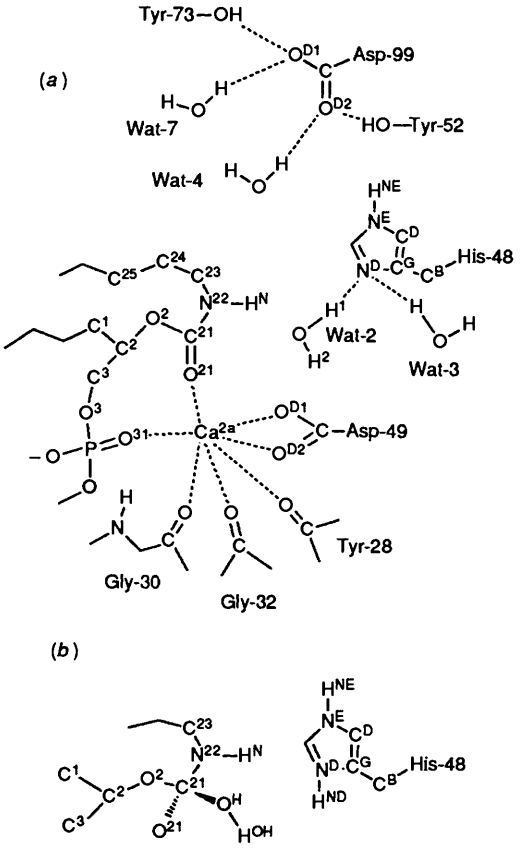

Fig. 3 (*a*) Atom labelling for active-site residues. (Atom labels of amino acids follow those in AMBER.) (*b*) Additional labels for oxyanion system.

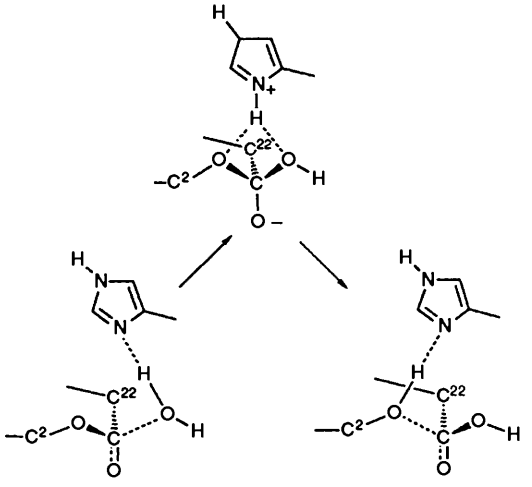

Fig. 4 Schematic representation of the reaction path for proton transfer for ester hydrolysis by PLA2

found to be unstable during MM minimisation of a full-sized phospholipid oxyanion, in that the system achieves a minimum at an H^{ND}–O^2 distance of 3–4 Å.[2] Therefore the doubly hydrogen-bonded intermediate was modelled with the use of constraints to enforce the two hydrogen bonds; after minimisation, the constraints were removed, and the structure was allowed to relax into the first local potential energy minimum.

QM–MM Calculations.—The structures of the PLA2–substrate complex were simplified for the MO calculations, in which the barrier to hydrolysis of the carbamate substrate was evaluated. A model of about 1000 atoms was constructed, which comprised 68 amino acid residues within 15 Å of the active site, and 50 water molecules. (This was equivalent to the models employed for the earlier investigation of ester and amide hydrolysis.)[2] A small number of atoms were treated explicitly in the MO calculations, while all other atoms were represented in the MO calculations as a field of atom-centred partial point charges. The QM atoms comprised the side-chains of His-48 and Asp-99 (modelled by imidazole and acetate, respectively), the nucleophilic water, and a fragment of the substrate (atoms C^2–C^{23}).

The structure of this QM model was taken directly from the MM-minimised complex, with the exception that the active-site residues were first refined so that their geometries were consistent with QM-optimised geometries. Thus the C^2–C^{23} fragments of the carbamate and oxyanion were refined by means of a hybrid QM–MM optimisation. This followed the methodology of Singh and Koilman's program QUEST, and we have described our modifications to this program elsewhere.[3] In brief, the wavefunction of the QM molecule (in this case, the C^2–C^{23} fragment) is evaluated within the field of point charges which represent the atoms of the environment, from which may be calculated the QM gradients of the QM atoms. To these are added the MM gradients imposed by the surrounding MM atoms. These arise from the standard AMBER MM forces, in terms of van der Waals non-bonded interactions, and also certain bond, angle and dihedral forces across the QM–MM junctions. The geometry optimisation of the QM atoms then proceeds by standard analytic gradient methods, except that the combined QM–MM gradients are employed. The MM environment remains static while the QM atoms are optimised to convergence. Note that the valency of the QM molecule is completed by a 'junction' hydrogen atom at each QM–MM junction; this hydrogen does not experience any MM forces, although it does interact with the field of charges. Unlike the original QUEST methodology, all QM atoms interact with exactly the same field of point charges: all the MM charges are retained, with the exception of the carbon atoms which are replaced by junction hydrogen atoms.

After the optimisation of the substrate fragment (with a 3-21G basis set), a final refinement was made to certain active-site residues. An MM minimisation was used to impose *in vacuo* QM geometries on the side-chains of His-48 and Asp-99, and to allow any necessary re-positioning of the water molecules and tyrosine hydroxy groups which are directly hydrogen-bonded to these residues. The result of these refinements was to produce a model in which the intramolecular geometries of the QM residues were consistent at a QM level, while intermolecular geometries were determined by the more approximate MM method.

Evaluation of MO Supermolecule Systems.—Single-point *ab initio* MO calculations were performed on the supermolecule systems within GAMESS with a 4-31G basis set, in order to evaluate the barrier to the formation of the oxyanion both *in vacuo* (with no environment present) and *in situ* (with the inclusion of the point charges of the MM atoms in the one-electron Hamiltonian). In the latter case, the standard AMBER charges were used, with the omission of very small charges ($< \pm 0.01$ e) and charges positioned very close to the QM system (*i.e.* the charges of methylene groups adjacent to the QM–MM junction). The following supermolecules were considered:

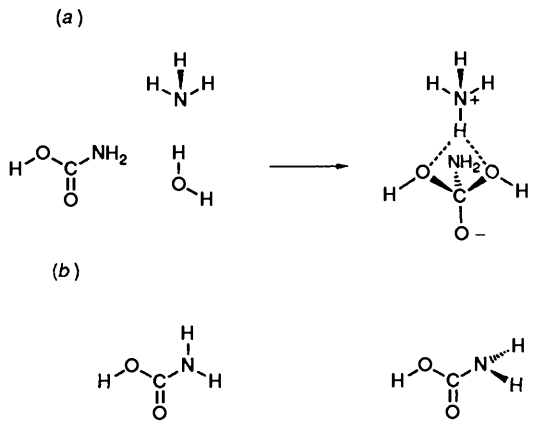

Fig. 5 (*a*) Supermolecule for the evaluation of the basis set dependency of carbamic acid hydrolysis *in vacuo*. An *in situ* model included a single point charge of +1 positioned 3 Å from the carbonyl oxygen, at an angle of 180° to the carbonyl. (*b*) Planar and non-planar conformations of carbamic acid.

Carbamate + water + imidazole + acetate ⟶
oxyanion + imidazolium + acetate

and were treated both *in vacuo* and *in situ*. For the *in situ* model, the MM energy of interaction between the QM supermolecule and the MM atoms of the bulk environment was also evaluated, again in terms of standard MM bonded and non-bonded energies (but without the electrostatic term). This provided a measure of the steric interaction between the QM supermolecule and the active site.

Large Basis Set MO Calculations.—The 4-31G basis set was chosen for the above models as a compromise between the need to use as large a basis set as possible, and the need to include explicitly a large number of active-site atoms. The limitations of this basis set are well known, and therefore it was decided to compare the 4-31G results with those obtained with a large polarised basis set (6-31G**) and with the estimation of electron correlation by second-order Moller–Plesset perturbation theory. The QM supermolecule was simplified to model the hydrolysis of carbamic acid, with His-48 represented by ammonia (Fig. 5). The substrate was modelled in planar and non-planar conformations. The calculations were performed for the supermolecule *in vacuo* and also in the presence of a +1 point charge, as a simple model of the calcium ion. For these systems, intermolecular geometries were chosen to approximate those within the enzyme, while internal geometries were obtained by STO-3G optimisations of the individual molecules.

Free-energy Perturbation Calculations.—The Gibbs free energy of binding of the carbamate substrate was evaluated by means of the free energy perturbation (FEP) method, as implemented in AMBER. As the observed binding energy of a substrate generally includes its desolvation energy, this was taken into consideration by means of the thermodynamic cycle[27] shown, where A(aq) is the solvated substrate and A(*in situ*) is the substrate bound to the active site. Measured binding energies of substates A and B are reflected in the values of ΔG_1 and ΔG_2. Computationally, it is easier to consider ΔG_3 and ΔG_4,

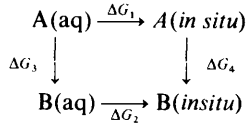

Table 1 STO-3G ESP charges for the FEP calculations on the carbamate, ester and amide phospholipids. For atom labels see Fig. 3.

Carbamate		Ester		Amide	
C^2	−0.092	C^2	−0.045	C^2	−0.257
H^2	+0.078	H^2	+0.068	H^2	+0.110
O^2	−0.401	O^2	−0.427	N^2	−0.416
—		—		H^N	+0.225
C^{21}	+0.890	C^{21}	+0.800	C^{21}	+0.561
O^{21}	−0.477	O^{21}	−0.438	O^{21}	−0.401
N^{22}	−0.534	C^{22}	−0.202	C^{22}	−0.031
H^{22}	+0.266	H^{22}	+0.058	H^{22}	+0.016
C^{23}	−0.135	C^{23}	−0.185	C^{23}	−0.258
H^{23}	+0.083	H^{23}	+0.058	H^{23}	+0.072

for the non-physical mutations which describe the perturbation of A into B either in a box of water or in the enzyme active site. Both of these perturbations can be achieved with minimal disruption to macromolecular structure and hence with a high reproducibility. The relative free energy of binding of A and B ($\Delta G_1 - \Delta G_2$) is equal to ($\Delta G_3 - \Delta G_4$).

For the calculation of solvation energies, small model substrates were solvated in a box of water, *e.g.* methyl propanoate and dimethyl carbamate for the ester ⟶ carbamate mutation. Charges were calculated by the ESP method with an STO-3G basis set, for STO-3G-optimised geometries (Table 1). A box of about 500 TIP3P water molecules was used to solvate the solute. The system was first heated to a temperature of 300 K with 1 ps of MD, and then equilibrated for 4 ps (2000 × 2 fs steps) at constant temperature (300 K) and pressure (1 atm), with the use of periodic boundary conditions and with an 8 Å non-bonded cut-off. Bond lengths were fixed to their force-field values during the simulation (to remove the high frequency bond stretches, and allow a larger step length to be taken).

For the FEP calculation, the 'window' method was used, by which the perturbation of the Hamiltonian of the ester into that of the carbamate was accomplished over a series of 21 discrete steps (windows).[18] Each window comprised 500 × 2 fs steps of MD to equilibrate the system, followed by 500 × 1 fs steps of data collection. At each window, ΔG is calculated for perturbations to the Hamiltonian in both forward and reverse directions, so that a single run yields the overall ΔG in both directions. The final conformation of the system was used to repeat the calculation in the reverse direction, in order to assess the dependency of the calculation on the initial solvent structure. Therefore ΔG is expressed as the mean of the four results obtained. The quoted standard deviation refers to the statistical reproducibility of the method and does not reflect errors in the force-field or in the choice of partial charges.

Free energies of binding to PLA2 were calculated for the full phospholipid substrates (ester, amide and carbamate). The ESP charges for the C^2–C^{23} fragment of each phospholipid were the same as those for the solvation calculation (Table 1). Charges for the remainder of the lipid were the same for all substrates.

The model comprised the whole enzyme, with initial coordinates taken from the MM minimisations. The solvent shells of these models were replaced by spherical caps of water molecules, of radius 15 Å from the C^2 carbonyl. To these were added five water molecules from the earlier models which were found to be hydrogen-bonded within the active site. A total of about 120 water molecules were present. During all MD, amino acid residues further than approximately 12 Å from the C^2 carbonyl were held fixed, so that some 46 residues, plus the calcium, substrate and water, were allowed to be mobile. This partial freezing of the enzyme is necessary if the entire enzyme is not to be fully solvated, and also prevents gross distortions of the enzyme during prolonged MD simulation. During MD, the

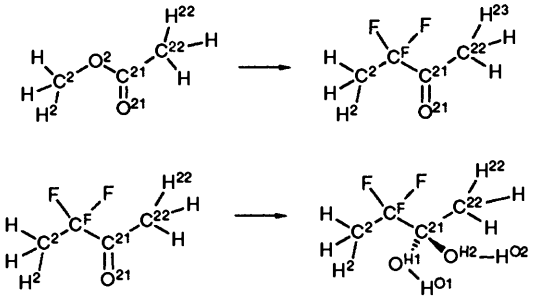

Fig. 6 Ester and fluorinated ketone solutes considered in the FEP calculations. Top, ester ⟶ ketone; below, ketone ⟶ hydrate.

Table 2 STO-3G ESP charges for the calculations of ester ⟶ ketone/hydrated ketone. For atom labels see Fig. 6.

Ketone		Hydrate	
C^2	−0.556	C^2	−0.474
H^2	+0.147	H^2	+0.125
C^F	+0.512	C^F	+0.506
F	−0.212	F	−0.222
C^{21}	+0.493	C^{21}	+0.654
O^{21}	−0.346	O^{H1}	−0.554
—		H^{O1}	+0.314
—		O^{H2}	−0.553
—		H^{O2}	+0.314
C^{22}	−0.555	C^{22}	−0.470
H^{22}	+0.145	H^{22}	+0.116

water molecules are prevented from drifting further than 15 Å from the C^2 carbonyl by means of a harmonic potential of 0.5 kcal mol^{-1} $Å^{-2}$ (this is necessary as periodic boundary conditions could not be used because of the size of the system).

The solvated PLA2–substrate system was initially minimised to improve the structure of the solvent shell. As before, the system was equilibrated at 310 K with MD. The FEP calculation was again performed by the window method (21 windows of 500 × 2 fs steps of equilibration plus 500 × 1 fs steps of data collection).

The results of the FEP calculations were found to be greatly in excess of known experimental values, and this was attributed to the neglect of intramolecular interaction energies within the phospholipids. In AMBER, the free energy is calculated from the intermolecular interactions between the defined substrate and the environment. Although the assumption is generally made that intramolecular interactions can be ignored, this may not be the case for these phospholipid substrates. Here there is a significant coulombic interaction between the C^2 carbonyl and the C^3 phosphate group; the neglect of this interaction would result in the environment of the calcium binding-loop bearing too positive a charge, and hence an exaggerated binding affinity of the carbonyl to the calcium would be expected.

The intramolecular interactions within the phospholipid were taken into consideration in a further series of FEP calculations, in which the phospholipid was divided into several fragments (defined as 'residues' within AMBER). Two partitions of the substrate were compared. In the first, the 'substrate' was redefined as only the C^2–C^{23} fragment of the lipid: the remainder of the lipid was therefore included within the bulk environment. In a second partition, the substrate was defined as the whole of the C^1 and C^2 chains, and only the C^3 phosphoryl ethylammonium chain was excluded.

Free Energies of Binding of Fluorinated Phospholipids.—Free energies of solvation and binding were evaluated in a similar manner for a fluorinated ketone phospholipid and its proposed hydrated form. The solvation energies of a model fluorinated ketone and its hydrate (Fig. 6) were calculated relative to methyl ethanoate. ESP charges were calculated with the STO-3G basis set at 3-21G-optimised geometries (Table 2). Solvation energies were calculated as before, although to improve the accuracy of the sampling, the FEP calculation was performed for double the periods of equilibration and data collection (*i.e.* with 1000 × 2 fs and 1000 × 1 fs steps of MD respectively, per window). The boxes of water contained approximately 290 water molecules for the perturbations of hydrate ⟶ ketone and ester ⟶ ketone.

For the calculation of binding energies within the active site of PLA2, a fluorinated ketone phospholipid was modelled, in which the O^2 oxygen of the ester was replaced by the difluoromethylene group. These calculations followed the same method as the earlier FEP calculations, with the interaction energies evaluated for the interaction of the whole phospholipid with the enzyme. Force-field parameters for fluorine were adapted from the CHARMM force-field.[28]

Three perturbations were performed, to check the self-consistency of the results: ester ⟶ ketone; ketone ⟶ hydrate; hydrate ⟶ ester. Initial MM minimisations demonstrated that the ketone and hydrate were both weakly bound to the active site, and did not stay bound to calcium during the MD simulation. Therefore to compare the relative binding energies of these substrates it was necessary to use constraints to keep the C^2 carbonyl in close contact with the calcium ion. Therefore, a dummy bond was defined between the carbonyl oxygen and the calcium. of length 2.5 Å and a force constant of 5 kcal mol^{-1} $Å^{-2}$, which was sufficiently weak to allow some stretching of the oxygen–calcium bond (up to approximately 3.5 Å) during the course of the MD. (The calcium ion was constrained to its initial position using a force constant of 5 kcal mol^{-1} $Å^{-2}$.) The perturbations were again performed over 21 windows, with 500 × 2 fs steps of equilibration and 500 × 1 fs steps of data collection at each window.

The reproducibility of the FEP calculations was seen to be poor, in particular for those perturbations which involved the hydrate. In order to improve the reproducibility of the results, the 'double-decoupled' method was used for the ketone ⟶ hydrate mutation. In this method, two separate perturbations are carried out.[18] In the first, the electrostatic parameters are perturbed while the van der Waals parameters are kept constant; this is followed by a second perturbation in which the van der Waals parameters are perturbed while the electrostatic parameters are constant.

MO Models of Substrate Binding and Polarisation.—A series of MO calculations were performed to investigate the relative binding energies of the ester, amide and carbamate substrates to calcium. In particular, the calculations assess the degree of polarisation of the substrate by the calcium ion and by the solvent, in order to determine the appropriateness of using *in vacuo* ESP charges to model a molecule which is considerably polarised by the environment.

In these MO calculations, the interaction energy was calculated for the binding of a small model substrate (formic acid, formamide or carbamic acid) to a single point charge. By the use of a small fractional point charge to model calcium (*e.g.* +0.5), it was possible to obtain a difference in the binding energies of the acid and amide which was of a similar magnitude to that expected *in situ* (*i.e.* a few kcal mol^{-1}). For each substrate, the point charge was placed 2.5 Å from the carbonyl oxygen, at an angle of 180°, to approximate the position of the calcium *in situ*.

To obtain an estimate of the degree of polarisation of the substrate by the point charge, the converged molecular orbitals

Table 3 (*a*) Selected interatomic distances/Å within the active site of PLA2 (after final QM–MM optimisations) for the complexes with the carbamate substrate (CAR1) and the oxyanion (OXY). (*b*) Selected distances for conformations CAR2 and CAR3. Atom labels are described in Fig. 3. CAL refers to the calcium ion.

(*a*)	CAR1	OXY
Environment of substrate		
O^{21}(SUB)-CAL	2.50	2.21
O^{21}(SUB)-H^{N}(Gly-30)	2.03	2.02
O^{31}(SUB)-CAL	2.21	2.23
C^{21}(SUB)-N^{D}(His-48)	4.22	3.21
C^{21}(SUB)-O(Wat-2)	2.98	—
O^{H}(SUB)-H^{ND}(His-48)	—	1.80
O^{2}(SUB)-H^{ND}(His-48)	—	2.08
O^{D1}(Asp-49)-H^{2}(Wat-2)/H^{OH}(SUB)	1.76	1.72
Hydrogen bonds of His–Asp		
N^{D}(His-48)-H^{1}(Wat-2)	1.92	—
H^{NE}(His-48)-O^{D2}(Asp-99)	1.69	1.62
O^{D2}(Asp-99)-H^{OH}(Tyr-52)	1.82	2.28
O^{D2}(Asp-99)-H(Wat-4)	1.80	1.76
O^{D1}(Asp-99)-H^{OH}(Tyr-73)	1.68	1.71
O^{D1}(Asp-99)-H(Wat-7)	1.72	1.80
(*b*)	CAR2	CAR3
Environment of calcium		
CAL-O(Tyr-28)	2.31	2.32
CAL-O(Gly-30)	2.32	2.38
CAL-O(Gly-32)	2.42	2.48
CAL-O^{D1}(Asp-49)	2.29	2.28
CAL-O^{D2}(Asp-49)	2.33	2.38
Environment of substrate		
O^{21}(SUB)-CAL	3.09	2.33
O^{21}(SUB)-H^{N}(Gly-30)	1.92	3.80
O^{31}(SUB)-CAL	2.21	2.23
C^{21}(SUB)-N^{D}(His-48)	4.18	4.32
C^{21}(SUB)-O(Wat-2)	2.95	3.50

Table 4 Selected dihedral angles/° for the carbamate substrate after initial MM minimisation of the PLA2–carbamate complex, for the conformations CAR1–CAR3. Atom labels are described in Fig. 3.

Angle	CAR1	CAR2	CAR3
C^{2}–O^{2}–C^{21}–O^{21}	−0.9	−20.4	−13.0
C^{2}–O^{2}–C^{21}–N^{22}	174.8	155.0	158.2
O^{2}–C^{21}–N^{22}–C^{23}	−103.9	−143.7	−128.9
O^{21}–C^{21}–N^{22}–H^{N}	−152.8	−175.3	−173.0
C^{21}–N^{22}–C^{23}–C^{24}	67.3	80.0	85.4
N^{22}–C^{23}–C^{24}–C^{25}	176.4	175.5	178.4

calculated for the substrate *in vacuo* were used as the initial orbitals for the calculation in the presence of the point charge. From the energy of the first cycle of the self-consistent field (SCF) calculation may be calculated the interaction energy of the unpolarised wavefunction with the point charge. The difference between the first and the final iteration of the SCF represents the stability which is a result of the induced polarisation by the point charge. The binding energy and degree of polarisation were evaluated at a variety of basis sets (STO-3G, 4-31G, 6-31G*) to investigate the basis set dependency of the results.

A similar procedure was followed to assess the degree of polarisation induced by bulk solvent. The substrates considered were methyl propanoate and dimethyl carbamate. Each was surrounded by a shell of 150 TIP3P water molecules, which was refined by MM minimisation while the substrate was held fixed at its QM-optimised geometry. The QM energy of each system was evaluated in a single-point MO calculation, in which the atoms of the water molecules were represented as a set of point charges in the one-electron Hamiltonian (the charge on the oxygen was −0.834).

Results and Discussion

MM Modelling of PLA2–Carbamate Complexes.—The structure of the minimised PLA2–carbamate complex was found to be very similar to those obtained for the ester and amide analogues in our earlier papers, with minimal distortion of the enzyme or the substrate. The phospholipid (conformation CAR1) was found to retain the extended conformation characteristic of phospholipids within the cell membrane, except for some rotation of the C^{3} chain to enable the phosphoryl moiety to bind to the calcium ion. The final structure is in agreement with the Verheij mechanism: the C^{2} carbonyl is bound to the calcium ion and to the -NH of Gly-30, and is within 3 Å of the nucleophilic water molecule, which is hydrogen-bonded to His-48. The C^{2} alkyl chain interacts with the hydrophobic wall of the active site. Selected interatomic distances are presented in Table 3(*a*).

Since these calculations were performed, a crystal structure of an amide phospholipid inhibitor bound to the active site of PLA2 has become available.[7] This structure is essentially similar to those discussed here, with the principal exception that the nucleophilic water is absent and the amide -NH is hydrogen-bonded to N^{D} of His-48. The displacement of the water may well be favoured by the formation of the hydrogen bond between the amide and His-48, but no analogous hydrogen bond would form in the case of ester or carbamate substrates.

The conformation CAR1 of the carbamate is therefore able to achieve a mode of binding exactly analogous to that of the ester and amide phospholipids: hence the difference in reactivity of these substrates is seen to be a function of the ester/amide linkage and does not arise because of any significant difference in the alignment of the carbonyl with the catalytic network in the active site.

As mentioned above, the torsional kink in the C^{2} chain of the original ester substrate was reproduced in the carbamate (conformation CAR1), with the result that the amide linkage is distorted away from planarity (see Table 4). Therefore the effects of imposing planarity were investigated in two further models. Conformation CAR2 was generated by MM minimisation of a planar starting conformation. The C^{2}–C^{23} fragment was now slightly wider, such that an unfavourable steric interaction arose between the C^{2} chain and the hydrophobic wall, which resulted in the displacement of the C^{2} carbonyl from the calcium ion (hydrogen bonding to Gly-30 was retained). The calcium–carbonyl distance was increased from 2.5 Å to 3.1 Å, which was found to have a significant effect on the energetics of hydrolysis of the carbamate.

For the final model of the carbamate reactant, molecular dynamics was used to search for a more favourable mode of binding of a planar carbamate. A conformation was obtained (CAR3) in which tight binding was achieved to the calcium (a carbonyl–calcium distance of 2.4 Å). This was the result of a small degree of translation of the substrate away from the hydrophobic wall of the active site, which enabled the carbonyl to move slightly closer towards the calcium, although with the loss of the hydrogen bond to Gly-30. In general, conformation CAR3 is very similar to the previous conformations. The amide linkage still shows a small degree of distortion away from planarity, as a close steric interaction with the wall of the active site is a consequence of the binding to calcium. Selected interatomic distances within the active site are presented in Table 3(*b*).

Table 5 Geometries of the carbamate substrate headgroup after optimisation *in situ* by the hybrid QM–MM method, at a 3-21G basis set. For comparison geometries are included for dimethyl carbamate optimised *in vacuo* in a planar conformation.

	in vacuo	CAR1	CAR2	CAR3
Lengths/Å				
C^2–O^2	1.450	1.452	1.457	1.461
O^2–C^{21}	1.356	1.346	1.362	1.346
C^{21}–O^{21}	1.213	1.222	1.218	1.221
C^{21}–N^{22}	1.341	1.373	1.340	1.351
N^{22}–H^N	0.995	1.002	0.998	0.999
N^{22}–C^{23}	1.461	1.487	1.468	1.476
Angles/°				
C^2–O^2–C^{21}	117.0	121.3	116.8	118.1
O^{21}–C^{21}–O^2	123.3	122.5	122.2	123.1
O^{21}–C^{21}–N^{22}	125.8	129.0	128.1	126.6
O^2–C^{21}–N^{22}	110.9	108.5	109.7	110.2
C^{21}–N^{22}–C^{23}	120.5	121.2	122.9	118.8
C^{21}–N^{22}–H^N	118.4	109.4	114.0	112.7
Dihedrals/°				
C^2–O^2–C^{21}–N^{22}	180.0	167.7	147.2	153.9
C^2–O^2–C^{21}–O^{21}	0.0	−11.8	−31.6	−22.4
O^2–C^{21}–N^{22}–C^{23}	180.0	−108.2	−148.9	−131.4
O^{21}–C^{21}–N^{22}–H^N	180.0	−157.7	−179.4	−176.5

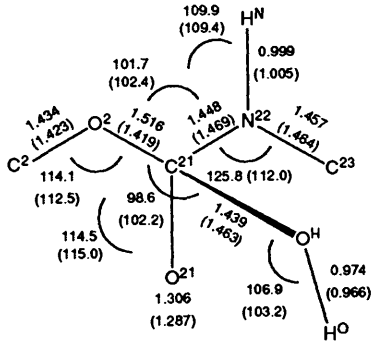

Dihedrals (°)		
C^2—O^2—C^{21}—N^{22}	103.9	(172.6)
C^2—O^2—C^{21}—O^{21}	−26.8	(45.2)
C^2—O^2—C^{21}—O^H	−147.9	(−78.1)
O^2—C^{21}–O^H—H^O	70.9	(142.4)
O^2—C^{21}–N^{22}—C^{23}	−131.5	(−77.5)
H^N—N^{22}–C^{21}—O^{21}	136.6	(175.0)

Fig. 7 Geometries of the carbamate oxyanion fragment, obtained with a 3-21G basis set. Values without parentheses are for the QM–MM optimisation *in situ*, while for comparison, values within parentheses are for an optimisation of the oxyanion *in vacuo*. Lengths are quoted in angstroms, angles in degrees.

The carbamate oxyanion was found to adopt a conformation which was again very similar to that found for the oxyanions of the ester and amide phospholipids. (Note that only one conformation of the oxyanion was modelled.) As described earlier,[2] constraints were imposed in order to obtain an oxyanion which was doubly hydrogen-bonded to His-48. This was achieved with minimal distortion of the structure of the active site or of the oxyanion. As proposed in our previous papers, such a doubly hydrogen-bonded oxyanion is required in order to achieve facile proton transfer from the nucleophilic water *via* His-48 to O^2, and has been found to be a stable minimum in calculations on the hydrolysis of a small ester substrate.[3] To achieve this conformation, the phospholipid reactant must move further into the active site towards His-48 and the nucleophilic water. As this results in an increase in steric hindrance, the doubly hydrogen-bonded oxyanion is not found to be a stable minimum in the MM calculations.

Table 6 ΔE_{QM} and $E_{MM/QM}$ (kcal mol^{-1}) for carbamate hydrolysis, at a 4-31G basis set. The supermolecule of dimethylcarbamate–imidazole–acetate is treated both *in vacuo* and *in situ* (the latter including the field of MM charges). The three carbamate conformations (CAR1–CAR3) are described in the text. ΔE_{QM} is the relative QM energy between the oxyanion supermolecule and the reactant supermolecule. $E_{MM/QM}$ is the MM interaction between the QM supermolecule and the MM atoms; ΔE_{TOT} is the sum of $\Delta E_{MM/QM}$ and ΔE_{QM}. Energies for ester and amide hydrolysis are quoted from ref. 2 for comparison.

Substrate		ΔE_{QM}	$\Delta E_{MM/QM}$	ΔE_{TOTAL}
CAR1	*in vacuo*	+16.0		
	in situ	−7.7	+8.4	+0.7
CAR2	*in vacuo*	+28.3		
	in situ	−9.3	+9.5	+0.2
CAR3	*in vacuo*	+26.1		
	in situ	+3.6	+5.1	+8.6
Ester	*in vacuo*	+19.1		
	in situ	−8.0	+8.0	0.0
Amide	*in vacuo*	+37.0		
	in situ	+22.9	+5.1	+28.0

Results of QM–MM Optimisations.—In this paper the hybrid QM–MM method has been used to optimise the geometry of a fragment of the carbamate and oxyanion within the active site, in order to describe the influence of the active site on the structure of the substrate. Table 5 and Fig. 7 detail the geometries of these fragments, and demonstrate that although the geometries are similar to those derived *in vacuo*, there are minor distortions to lengths and angles attributable to the strong electrostatic interaction with calcium, and, as a result, the *in situ* structures are several kcal mol^{-1} higher in energy than the *in vacuo* structures. In particular, the carbonyl bond is stretched, with some shortening of adjacent bonds. This is well demonstrated in the carbamate substrates, where the degree of distortion of the carbonyl geometry can be related to the tightness of binding to the calcium (*i.e.* the carbamates bind in the order CAR3 > CAR1 > CAR2).

For the oxyanion, there is a similar degree of distortion from the *in vacuo* structure. Note that the position of the hydroxy group is now dictated by a hydrogen bond to a carboxylate oxygen of Asp-49, ligand of calcium.

Energetics of Carbamate Hydrolysis.—The same supermolecule models have been considered for carbamate hydrolysis as were described for ester and amide hydrolysis in a previous paper.[2] As before, the difference in QM energy between the oxyanion supermolecule and the reactant supermolecule is taken as a measure of the barrier to formation of the oxyanion. This is not intended as an accurate approach to derive the absolute rate of substrate hydrolysis, but rather as a practical method to describe quantitatively relative energetics between different substrates, or between different environments.

The results for all the substrates are compared in Table 6. Note that each of the three carbamate reactants has been compared against the same model of the oxyanion intermediate. In brief, the results for ester and amide (which are quoted from ref. 2) demonstrate that the barrier to amide hydrolysis is greater than that of ester hydrolysis in the *in vacuo* model, which is to be expected from the resonance stability of the amide linkage. The addition of the point charge field (to represent the bulk active-site environment) results in a large decrease in ΔE_{QM}, which is sufficient to remove the barrier to ester

Table 7 4-31G Mulliken populations for the carbamate carbonyls of the carbamate–imidazole–acetate supermolecules. Populations for the ester and amide are quoted from ref. 2 for comparison. Atom labels are described in Fig. 3.

			Atomic Mulliken populations					
Substrate			H^N	O^2	C^{21}	O^{21}	N^{22}	H^N
Carbamate								
CAR1	*in vacuo*	Reactant		−0.76	+1.06	−0.61	−0.77	+0.36
		Oxyanion		−0.80	+0.99	−0.83	−0.82	+0.31
	in situ	Reactant		−0.75	+1.14	−0.80	−0.77	+0.36
		Oxyanion		−0.82	+1.09	−1.07	−0.82	+0.32
CAR2	*in vacuo*	Reactant		−0.75	+1.11	−0.65	−0.84	+0.38
	in situ	Reactant		−0.77	+1.17	−0.75	−0.85	+0.37
CAR3	*in vacuo*	Reactant		−0.75	+1.06	−0.64	−0.79	+0.37
	in situ	Reactant		−0.75	+1.16	−0.81	−0.80	+0.36
Ester	*in vacuo*	Reactant		−0.73	+0.81	−0.61		
		Oxyanion		−0.81	+0.82	−0.84		
	in situ	Reactant		−0.71	+0.88	−0.80		
		Oxyanion		−0.81	+0.89	−1.09		
				N^2				
Amide	*in vacuo*	Reactant	+0.35	−0.85	+0.78	−0.65		
		Oxyanion	+0.29	−0.84	+0.74	−0.84		
	in situ	Reactant	+0.37	−0.85	+0.84	−0.85		
		Oxyanion	+0.30	−0.85	+0.81	−1.09		

hydrolysis. This highlights the major role of the electrostatic interactions between the oxyanion, the calcium ion and the ionic His–Asp couple in the stabilisation of the oxyanion. (Our earlier calculations demonstrated that the loss of the ionic His–Asp couple, by means of a putative second proton transfer from His-48 to Asp-99, significantly destabilises the formation of the oxyanion.)[2] However, the addition of the environment has a greater effect on the stabilisation of ester hydrolysis than on amide hydrolysis. This arises from the larger binding energy of the amide substrate to the calcium, compared with the ester substrate, which thereby reduces the stabilisation of the amide oxyanion relative to the amide reactant. The MM energy of interaction between the QM supermolecule and the environment ($E_{MM/QM}$) represents a small steric (van der Waals) destablisation of the oxyanion by the active site, as well as some increase in MM torsional energy within the oxyanion.

For the carbamate analogues, it is seen that the barrier to carbamate hydrolysis for the original non-planar carbamate, CAR1, *in vacuo*, is similar to that of the ester, and significantly less than the amide. The addition of the environment of the active site reduces this barrier by an extent similar to that observed in the case of ester hydrolysis. Overall, the carbamate inhibitor appears to be more readily hydrolysed than the ester. This is contrary to the expected behaviour of the carbamate, which should be approximately as resistant to hydrolysis as the amide, because of the π-electron delocalisation over the amide linkage. However, in this model the carbamate is in a conformation where the planarity of this system is significantly disrupted and resonance stabilisation has been lost.

From Table 6 it is seen that the barriers to hydrolysis *in vacuo* of the planar conformations, CAR2 and CAR3, are of a similar magnitude, and are larger than for CAR1, which reflect the resonance stabilisation of the planar carbamate. The *in situ* model highlights the poor binding of CAR2 relative to CAR3. Thus the barrier to the hydrolysis of conformation CAR2 is significantly reduced because of the destabilisation of the CAR2 substrate relative to the oxyanion. The environment of the active site stabilises the *in vacuo* ΔE_{QM} by 37.6 kcal mol^{-1} for CAR2, compared with 23.7 and 22.5 kcal mol^{-1} for CAR1 and CAR3 respectively. As CAR1 and CAR3 have similar binding energies, the difference in reactivity between CAR1 and CAR3 which is seen *in vacuo* is retained *in situ*.

It is known that the carbamate substrate is an inhibitor of PLA2.[29] The above calculations demonstrate that the carbamate phospholipid is unlikely to bind in the conformation CAR1 (a similar conformation to the ester lipid) because the loss of planarity of the C^2 headgroup facilitates hydrolysis of the carbamate. For the planar carbamates, CAR2 and CAR3, ΔE_{QM} is dependent on the binding energy of the carbamate headgroup. The weak binding of CAR2 results in a larger decrease in ΔE_{QM}. Although it cannot be dismissed that CAR2 is the true mode of binding of the carbamate, it would be necessary for both the ester and amide lipids to bind similarly to CAR2, to maintain the differences in reactivity of the three substrates. It is also possible that the carbamate binds in the manner of CAR2 but then experiences an additional unfavourable barrier in the formation of the oxyanion intermediate.

Mulliken populations for the carbamate are given in Table 7. These demonstrate the dependency of the polarisation of the carbonyl bond on the planarity of the carbamate (*in vacuo*), and on the tightness of binding to calcium *in situ*.

Basic Set Dependency of Carbamate Results.—The barrier to the formation of the oxyanion was investigated in a simpler *in vacuo* model, in which His-48 was replaced by ammonia, and the carbamate by carbamic acid. In our earlier report,[2] we used a similar model to investigate the basis set dependency of ester and amide hydrolysis, using formic acid and formamide as the substrates, and it was observed that there were significant discrepancies between the 6-31G**/MP2 results and those at the 4-31G and 6-31G** basis sets. For both acid and amide substrates, ΔE_{QM} was increased significantly as the basis set was increased from 4-31G to 6-31G** basis sets (by approximately 20 kcal mol^{-1} for formic acid, and 11 kcal mol^{-1} for formamide), while the inclusion of electron correlation decreased ΔE_{QM} (by 9 and 13 kcal mol^{-1} for formic acid and formamide, respectively). Thus it was seen that the addition of electron correlation partly cancelled the effect of polarisation functions. Overall, the discrepancy between 4-31G and 6-31G**/MP2 was small for formamide (−2 kcal mol^{-1}) while it was more significant for formic acid (+11 kcal mol^{-1}). Hence the 4-31G basis set underestimates the barrier to ester hydrolysis, and exaggerates the relative rates of ester and amide hydrolysis.

Similar calculations are here reported for the carbamic acid

Table 8 Basis set dependency of the hydrolysis of carbamic acid (carbamic acid + water + ammonia ⟶ oxyanion + ammonium, *in vacuo*, as in Fig. 5); the *in situ* model includes a +1 point charge to mimic the calcium ion. Two carbamic acid substrates are considered, planar and non-planar. Energies are calculated at the same geometry for formamide and formic acid hydrolysis at 4-31G for comparison. ΔE_{QM} in kcal mol^{-1}.

	Carbamic acid			
Basis	Planar	Non-planar	Formic acid	Formamide
in vacuo				
STO-3G	+95.4	+91.3		
4-31G	+59.7	+40.9	+41.9	+59.8
6-31G**	+72.7	+58.7		
6-31G**/MP2	+62.2	+49.7		
in situ				
STO-3G	+72.6	+66.7		
4-31G	+44.9	+24.6	+22.8	+47.1
6-31G**	+56.3	+40.8		
6-31G**/MP2	+45.9	+31.8		

substrate. These calculations also investigate the relative barrier to hydrolysis of planar and non-planar substrates. As the intermolecular geometries of these supermolecules were slightly different from those described in ref. 2, the formic acid and formamide models are repeated here at the new geometry (at 4-31G only).

Table 8 presents ΔE_{QM} for carbamic acid hydrolysis at a range of basis sets, and for formic acid and formamide hydrolysis for comparison. The disruption of the planarity of the amide linkage in carbamic acid has a large effect on ΔE_{QM}. The planar carbamate is found to have a similar barrier to the amide (ΔE_{QM} of +59.7 and +59.8 kcal mol^{-1} for carbamate and amide respectively, *in vacuo*, at 4-31G) while the non-planar carbamate is similar to formic acid (ΔE_{QM} of +40.9 and +41.9 kcal mol^{-1} for carbamate and formic acid respectively). The non-planar carbamic acid is expected to be more readily hydrolysed than formic acid, as the electron-withdrawing effect of the nitrogen atom polarises the carbonyl to assist nucleophilic attack and assists in the delocalisation of the negative charge of the oxyanion.

It is seen that ΔE_{QM} is significantly increased on the addition of polarisation functions (*i.e.* on going from 4-31G to 6-31G**), but that this is partly reversed on the inclusion of electron correlation (MP2). Because of this, the 4-31G and 6-31G**/MP2 energies are very similar for the planar carbamate but show a large discrepancy for the non-planar carbamate, and thus follow the same trend which was seen for amide *versus* ester hydrolysis.

The relative binding energies of the reactants and the intermediates to the point charge determines the degree of stabilisation provided by the point charge. The binding energy of the carbamate oxyanion supermolecule to the point charge (−45.4 kcal mol^{-1}, 4-31G) is similar to that of the oxyanions of the acid (−44.8) and amide (−46.1). The binding energies of the reactants shows a marked progression: formic acid, −25.7; non-planar carbamate, −29.0; planar carbamate, −30.5; amide, −33.4 kcal mol^{-1}. Although the amide and the planar carbamate are seen to be equally resistant to hydrolysis *in vacuo*, carbamate hydrolysis is more strongly stabilised by the point charge and so a discrepancy in the relative rates arises *in situ*. This is because of the stronger binding of the amide reactant to the point charge, which results in the smaller relative stabilisation of the amide oxyanion relative to the amide reactant. Similarly, the non-planar carbamate is more readily hydrolysed than the acid *in vacuo*, but this difference is reversed in the presence of the point charge.

As in the comparison of ester *versus* amide energies, the limitations in the 4-31G basis set exaggerate the difference between the reactivity of planar and non-planar carbamates. Thus in the calculations discussed in the previous section, the difference in reactivity between substrates CAR1 and CAR3 will be overestimated by the 4-31G basis set. From the calculations on carbamic acid, the difference in barriers [ΔE_{QM}(planar) − ΔE_{QM}(non-planar)] is approximately +19 kcal mol^{-1} at 4-31G and +13 kcal mol^{-1} at 6-31G**/MP2, a discrepancy of approximately 6 kcal mol^{-1}. This figure is an estimation of the discrepancy for the comparison of carbamate substrates which are optimally planar and optimally non-planar. The differences in amide planarity between conformations CAR1–CAR3 are not so extreme, and therefore the error due to the use of the 4-31G basis set may not be so great.

Conclusions for Carbamate Hydrolysis.—The results of the MO calculations of planar and non-planar carbamate hydrolysis parallel those of ester and amide hydrolysis. The resonance stability of a planar amide linkage markedly increases the carbamate's resistance to hydrolysis *in vacuo*. *In situ*, however, carbamate hydrolysis is catalysed to an extent intermediate between that of ester and amide, and this is directly related to the binding energy of the carbamate. Note that although the carbamate is more polarised than the amide (in terms of Mulliken populations), it binds less strongly to calcium, presumably because of the large positive charge on the carbonyl carbon.

On binding to PLA2, it is unlikely that the carbamate adopts the conformation CAR1 (*i.e.* identical to the ester substrate) because of the loss of resonance stability of the amide linkage. However, because a planar carbamate is more bulky than CAR1, it is proposed that it may bind in a slightly different manner than the ester or amide in order to achieve a close carbonyl–calcium distance and hence a large binding energy; therefore conformation CAR3 may be preferred over CAR2.

These calculations are not intended as a method to calculate absolute rates of hydrolysis for these substrates. There are clearly too many approximations in the method for this to be feasible, for example in the choice of basis set, the description of the bulk environment, and the neglect of the contribution of entropy. However, some of these limitations may be overcome when the same model is applied to several substrates, so that relative differences in reactivity are investigated.

FEP Calculations of Carbamate Binding Energy.—Experimentally, quantitative estimates of relative binding energies to PLA2 are difficult to obtain. This is because PLA2 only has a significant affinity for aggregated (micellar) substrate. Therefore the experimental determination of binding kinetics is obscured when the critical micelle concentrations of the substrate and the inhibitor are dissimilar, or when the affinities of PLA2 for mixed

micelle and pure substrate are dissimilar.[4] However, the amide analogue is reported to bind more strongly than the ester, with approximately a 10-fold difference in the binding constant.[30] Data for the carbamate are again scarce, and no quantitative estimates are available for the binding affinity of the carbamate in relation to the ester or amide; as discussed later, all QM calculations on small test systems suggest that the carbamate should bind strongly but not as well as the amide.

The relative free energies of solvation for the mutation carbamate ⟶ ester was evaluated as $+2.40 \pm 0.36$ kcal mol^{-1} (*i.e.* the carbamate is more strongly solvated), which compares with a value of $+0.62 \pm 0.11$ kcal mol^{-1} for the analogous amide ⟶ ester mutation, described in ref. 2. The carbamate is more strongly solvated than either ester or amide because of the greater polarisation of the carbonyl bond and the presence of an extra hydrogen-bonding site.

For the interaction of the whole phospholipid with the active site of PLA2, the FEP calculation gave a very large binding energy for the carbamate ⟶ ester mutation of $+9.42 \pm 0.24$ kcal mol^{-1}. Although the carbamate is expected to bind strongly, this figure is clearly a large overestimation of typical experimental binding energies, even when the energy of desolvation is taken into consideration. The experimental binding affinity of the amide is about 10-fold greater than that of the ester,[30] which suggests a difference in ΔG of binding of only about 2 kcal mol^{-1}. (More recently a 1200-fold difference in binding energies was reported for a particular amide inhibitor, which achieves a conformation in which it is also hydrogen-bonded to His-48;[7] this additional interaction is not modelled in these calculations.)

The present point charge model of the system is perhaps inadequate in that the mutual induced polarisation of the substrate and the environment is ignored, and *in vacuo* charges are used for all atoms. This may be a significant factor in the overestimation of the binding energies: for example, the effective charge around the calcium ion will be too large because the polarisation of the oxygen ligands by the calcium is not represented.

However, there is a further failing in the current methodology which is more significant in the present example. As discussed earlier, ΔG is calculated from the interaction energy between the whole of the phospholipid substrate and the enzyme, while the intramolecular interactions within the substrate are ignored. In particular, the neglect of the electrostatic interaction between the C^2 carbonyl and the C^3 phosphate group may exaggerate the binding energy of the carbonyl to the calcium ion.

Therefore the FEP calculations were repeated with the phospholipid redefined to comprise several fragments (in terms of AMBER 'residues'). In the first partition, the C^2 ester linkage (atoms C^2–C^{23}) was defined as the substrate, with the remainder of the phospholipid included in the environment. The interaction energy of the C^2 carbonyl with the calcium ion is now much reduced. Thus, ΔG for amide ⟶ ester is $+3.12 \pm 1.0$, and for amide ⟶ carbamate is -1.47 ± 0.50 kcal mol^{-1} (note that the carbamate now apparently binds more strongly than the amide). A second partition was also evaluated, in which the whole of the C^2 and C^1 chains was defined as the substrate; ΔG for amide ⟶ ester is now $+0.80 \pm 0.10$, and amide ⟶ carbamate is -2.49 ± 0.99 kcal mol^{-1}. The difference in the results for the two partitions is probably not significant in view of the large variability.

Although the magnitude of these energies is more reasonable, this method of partitioning the substrate is not entirely satisfactory. The above energies are not only the interaction energies of the carbonyl fragment with the active site, but now also include the interaction of the fragment with the remainder of the substrate. These intramolecular interactions need to be included if they are different in the bound and the unbound substrate but should be excluded otherwise. (For example, the repulsive interaction of the C^2 carbonyl with the phosphate is expected to increase significantly when the phosphate group is positioned closer to the carbonyl on binding, whereas other interactions will be essentially the same in the unbound and the bound states.)

An approximate correction for the above energies is to calculate the solvation energy for the phospholipid using the same partition, so that the solvation energies also include all the intramolecular interactions. The solvation energies may then be subtracted from the *in situ* energies, so that only the *change* in intramolecular interaction is described. This was performed for the amide ⟶ ester and amide ⟶ carbamate mutations in both partitions considered above.

For the solvation calculations, a single amide phospholipid was initially assigned the X-ray conformation described by Hitchcock *et al.*[24] The phospholipid was solvated by a shell of water of 15 Å radius centred on the C^2 carbonyl (175 water molecules), as the phospholipid is too large to solvate readily in a periodic box, and the system equilibrated at 300 K for 4 ps of MD. The FEP calculation was performed over 11 windows, with each window consisting of 500 × 2 fs steps of equilibration and 500 × 1 fs steps of data collection. A 10 Å non-bonded cut-off was used.

The re-calculated solvation energies now include the intramolecular interaction of the C^2–C^{23} fragment with the rest of the phospholipid as well as the interaction with the water molecules. The electrostatic interaction between the C^2 fragment and the phosphate is found to be large even when the system is solvated. Thus for the partition of the C^2–C^{23} fragment: ΔG (amide ⟶ ester) $= -2.06 \pm 0.23$, ΔG (amide ⟶ carbamate) $= -9.80 \pm 0.71$; for the partition of the C^1 and C^2 chains: ΔG (amide ⟶ ester) $= -2.61 \pm 0.08$, ΔG (amide ⟶ carbamate) $= -10.21 \pm 0.62$ kcal mol^{-1}.

These results can be used to correct the *in situ* results. Thus, for the first partition, the net binding energy for amide ⟶ ester becomes $(+3.12 \pm 1.0) - (-2.06 \pm 0.23) = +5.2 \pm 1.2$, while for amide ⟶ carbamate it is $(-1.47 \pm 0.50) - (-9.80 \pm 0.71) = +8.3 \pm 1.2$ kcal mol^{-1}. For the second partition, the net binding energy for amide ⟶ ester becomes $(+0.80 \pm 0.10) - (-2.61 \pm 0.08) = +3.4 \pm 0.2$, while for amide ⟶ carbamate it is $(-2.49 \pm 0.72) - (-10.21 \pm 0.63) = +7.7 \pm 1.3$ kcal mol^{-1}. Thus both partitions give comparable results. While the amide is now the most strongly bound, the ester is seen to bind more strongly than the carbamate, although the variability is again large. Note also that the solvation energies assume that the C^2 carbonyl is fully solvated, while in the lipid membrane this may not be the case. This solvation of the carbonyl serves to reduce the net binding energy of the carbamate relative to amide and ester.

This correction for intramolecular interactions is not ideal. Clearly the simulation of a single phospholipid in a small quantity of solvent is a poor approximation of the *in situ* case of a bulk membrane in which each monomer has limited freedom of movement, and where interactions between monomers may be of some significance. More importantly, the intramolecular electrostatic interactions are calculated over short distances and hence are large and are likely to be subject to significant error. Thus, in the present model these results should be accepted as semi-quantitative at best.

MO Models of Substrate Binding.—A series of MO calculations was performed to investigate substrate binding to a single point charge (to represent calcium), in order to clarify the relative binding energies of ester, amide and carbamate, and to assess the degree of polarisation of the substrate by the charge.

The results (Table 9) demonstrate that binding energies and the degree of polarisation are dependent on the basis set, and

Table 9 QM interaction energies between small model substrates and a single point charge of +0.5 (to simulate calcium ion), *in vacuo*. Interaction energies (E_{int}) between substrate and point charge include polarisation of the substrate by the charge. E_{pol} represents the stabilisation of the wavefunction due to polarisation by the point charge. Energies in kcal mol^{-1}

Basis set		Formic acid	Formamide	Carbamic acid
STO-3G	E_{int}	−6.75	−9.97	−9.85
	E_{pol}	−0.70	−0.79	−0.76
4-31G	E_{int}	−11.09	−15.91	−14.32
	E_{pol}	−1.22	−1.34	−1.26
6-31G*	E_{int}	−10.16	−14.38	−13.43
	E_{pol}	−1.24	−1.36	−1.28

Table 10 Evaluation of QM interaction energies between ester (methyl propanoate) or carbamate (dimethyl carbamate) substrates with a field of point charges to represent a shell of AMBER water molecules. E_{int} is the interaction energy between the QM molecule and the point charges, and includes the effect of polarisation of the wavefunction by the charges. E_{pol} is the stabilisation of the solute due to polarisation by the field of charges. Energies in kcal mol^{-1}

Basis set		Ester	Carbamate	Difference (carbamate − ester)
STO-3G	E_{int}	−11.78	−14.96	−3.18
	E_{pol}	−0.81	−0.97	−0.16
4-31G	E_{int}	−19.56	−23.30	−3.74
	E_{pol}	−1.62	−1.80	−0.18

that the STO-3G basis again underestimates these effects in comparison to larger basis sets (4-31G, 6-31G*). However, the relative binding energies between substrates is fairly consistent across the basis sets. Therefore the use of STO-3G ESP charges is not expected to result in a significant discrepancy in the FEP calculation of relative binding energies for these systems. (It is worth noting that when large basis sets are used to calculate ESP charges, the charges are usually scaled down because these basis sets overestimate experimental dipole moments.)

The results confirm that the amide binds more strongly to the point charge than the carbamate. Although the carbonyl oxygen of the carbamate bears a large negative charge, this is countered by the large positive charge on the carbonyl carbon, and the net result is that the binding energy of the carbamate is intermediate between ester and amide. The polarisation of the substrates by the point charge is significant, but is relatively constant between substrates; the amide is polarised most, with the carbamate and ester polarised to a lesser extent. The relative differences in substrate polarisation do not affect significantly the relative binding energies; thus the use of 'unpolarised' ESP charges should give a reasonable description of relative binding energies. (The use of 'polarised' charges may be more important in the description of the active site, in particular the environment of the calcium ion, so that the shielding of the calcium is accurately represented.)

Similar results were seen in the model of ester and carbamate solvation, in which was calculated the interaction of the substrate with a field of charges which represented an MM-minimised box of water. The results are shown in Table 10. The interaction energies and the degree of polarisation are again seen to be larger at the level of the 4-31G than at the STO-3G basis set, and larger for the carbamate compared with the ester. Relative energies are seen to be similar regardless of basis set. Thus the carbamate binds more strongly to the solvent by 3.7 kcal mol^{-1} (4-31G) when compared with the ester, while the difference in polarisation amounts to only 0.2 kcal mol^{-1}. (These interaction energies exceed the desolvation energies calculated by the FEP method, in which approximately half of the interaction energy arises from electrostatic interactions, and the remainder from van der Waals interactions; but this may reflect that these MO calculations refer to a water structure which is minimised around the solute, and hence has a higher electrostatic interaction, while the FEP calculation uses a water structure at 300 K which is less tightly bound to the solute. Thus the degree of polarisation calculated here would be expected to exaggerate that which would be achieved at 300 K.)

These calculations suggest that the polarisation of the solute by the solvent is significant, but may be taken as approximately a constant for the ester and carbamate substrates.

FEP Binding Energies of Fluorinated Phospholipids.—The free energies of solvation for the small fluorinated ketone and its hydrate were evaluated for the perturbation of hydrate ⟶ ketone as +3.65 ± 0.60, and for ketone ⟶ ester as + 0.69 ± 0.26 kcal mol^{-1}. Thus the ester is seen to be slightly less strongly solvated than the ketone, as the extra hydrogen-bonding capacity provided by two fluorine atoms compensates for the poor polarisation of the carbonyl bond in the ketone. The hydrate is solvated to a much greater extent, because of the four extra hydrogen-bonding sites (*i.e.* two hydroxyl hydrogen atoms, and a hydroxyl oxygen; the oxygen tends to form two hydrogen bonds).

The perturbations of the full-sized fluorinated phospholipid inhibitors within the active site of PLA2 were subject to a larger variability. The FEP calculations yielded ΔG for the perturbation of ester ⟶ ketone = +3.93 ± 0.43; for hydrate ⟶ ester, ΔG = −5.81 ± 0.56; and for ketone ⟶ hydrate, ΔG = +1.00 ± 0.59 kcal mol^{-1}. The poorly polarised carbonyl of the ketone is seen to bind weakly to the calcium in comparison to the ester, while the hydrate binds still more weakly. During the course of the MD, the hydrate adopts a conformation where the hydroxyl hydrogen H^{O1} is attracted to the oxygen ligands of calcium, while the second hydroxyl hydrogen H^{O2} can achieve a hydrogen-bonding distance with N^{D} of His-48. The poor binding of the hydrate to the active site implies that the favourable interaction between the calcium and the hydroxyl oxygens (which bear a larger negative charge than in the ketone or ester) is outweighed by the repulsion between the hydroxyl hydrogen atoms and the calcium.

It was observed that the reproducibility of these calculations was comparatively poor, in particular for the calculations which involved the hydrate. This is most likely the result of the mobility of the hydroxy groups of the hydrate. These atoms have a large interaction energy with the calcium ion, and it may be that the significant rotational movement of the hydroxy groups causes very large fluctuations in the substrate–calcium interaction energy. (The mobility of the hydroxy groups will increase during the calculation, as they are mutated into atom-types which have progressively smaller steric and torsional parameters.) The interaction energy should of course be averaged during the FEP calculation, but the length of the MD simulation is probably insufficient to describe fully the conformational energy surface.

In order to try to improve the variability of the results, the decoupled calculation was performed. Here the mobility of the hydroxy groups should be reduced, because steric and electrostatic mutations are separated. Hence, for the example of hydrate ⟶ ketone, it is possible to retain the steric parameters of the hydroxy groups while their charges are mutated to zero. This method requires a second FEP run, where the steric parameters of the hydroxy groups are allowed to mutate to zero to complete the full perturbation of hydrate ⟶ ketone.

The results of the decoupled calculations were similar to

those above, with no improvement in variability. However, it is now apparent that the poor reproducibility is a function of the electrostatic interactions. Thus, for the perturbation of hydrate ⟶ ketone, ΔG(electrostatic) = -2.17 ± 2.1, while ΔG(van der Waals) = $+1.35 \pm 0.019$, to give ΔG(total) = -0.82 ± 2.1 kcal mol^{-1}. The total energy is similar to that obtained by the direct method; the standard deviation appears larger, but is probably a more accurate estimation of the true standard deviations of the simulation (*i.e.* the original results had a fortuitously low variability).

Note that the variability in these results does not arise from any large discrepancy between the forward and backward estimation of ΔG in a single run; the discrepancy arises between consecutive runs, because of the conformational dependency of the system. Therefore the variability is a reflection that the two perturbations are following somewhat different pathways, because of the difficulty in achieving sufficient sampling of the configurational surface during the course of the FEP calculation.

The FEP calculations for the fluorinated phospholipids are unsatisfactory for several reasons. Firstly, the inhibitors bind so weakly that the PLA2–inhibitor complex is unstable during MD simulation. Thus it is necessary to use constraints to retain close binding of the carbonyl to calcium, and hence it is probably not possible to get a true measure of the relative binding energies of the inhibitors, as the complex may be unrealistically stabilised. Secondly, the reproducibility of the hydrate mutations is comparatively poor; to achieve a better sampling of the configurational energy surface of the system would probably require a much longer MD simulation than has been used here. Finally, the assessment of intramolecular interactions within the phospholipid has been neglected.

The limitations in the methodology prevent the quantitative evaluation of relative binding energies between these fluorinated inhibitors. However, it is clear that neither the ketone nor its hydrate is capable of binding strongly to PLA2. Thus the strong binding which was observed experimentally for these fluorinated analogues is most likely due to an anionic inhibitor, such as a deprotonated form of the hydrate, which would resemble the oxyanion intermediate of phospholipid hydrolysis. Although the binding energy of such an oxyanion has not been quantified here by FEP calculations, it is clear from our earlier MO calculations that the interaction energy of the anionic species with the calcium would be very much larger than any of the perturbations evaluated above.

Conclusions

The MO model of ester and amide hydrolysis which was presented in ref. 2 has been applied to the investigation of the hydrolysis of a carbamate inhibitor of PLA2. The value of the model is that it is able to quantify the differences in reactivity of a range of substrates, and to suggest a mechanism whereby substrate specificity arises. The approximations in the methodology, in terms of the description of the bulk environment and the level of QM theory which has been used, limit the quantitative accuracy of the results, and therefore it is not intended to use such a model to predict the absolute barrier to hydrolysis of any substrate. However, it is hoped that valid comparisons can be made between substrates, and that in ideal cases these may approach quantitative accuracy.

Such a comparison is only possible if the substrates are treated in a similar manner, and therefore the same active-site model has been used to describe the bulk environment in each case. The computational method may be less suitable for molecules which are structurally very different from the natural phospholipids, *e.g.* those which cause significant distortion of the active site. However the model has been shown to be capable of describing subtle effects on the barrier to carbamate hydrolysis which are dependent on the conformation and binding energies of the substrate.

The basis set dependency of the results is seen to be considerable, and is not consistent between substrates (*e.g.* the discrepancy in the 4-31G estimates of ester *versus* amide energetics) or even within a substrate (*e.g.* planar *versus* non-planar carbamate energetics). However, it is not possible at present to apply post-Hartree–Fock methods to these large supermolecule systems, and therefore the most that can be done is to attempt to calibrate the 4-31G barriers by means of appropriate calculations on smaller systems at higher basis sets. The large basis set calculations reported here are seen to reproduce the essential features of reactivity which were observed at 4-31G.

The FEP method has been used to quantify relative free energies of binding among various substrates and inhibitors of PLA2, although at present there remain several practical limitations in the methodology. It is worth noting that PLA2 itself presents certain difficulties in the execution of the FEP calculation. The phospholipid monomer has considerable conformational mobility, even when bound within the active site, whereas most published studies look at rather more rigid substrates. Therefore it would be expected that equilibration of the PLA2–substrate system would be difficult to achieve. The calculation is also unrealistic because of the simulation of PLA2 in aqueous solution, rather than as a complex with the lipid membrane. The presence of the membrane would be expected to reduce the mobility of the active site residues and the substrate.

In conclusion, the present study demonstrates that although much useful information can be obtained from the application of MO and FEP methods to enzyme catalysis, there remain many approximations in the methodology which must be addressed if quantitative binding energies and rates of reaction are to be calculated. Therefore a valid approach at present is to use these theoretical models to compare similar systems in a similar fashion and thereby to reduce the intrinsic errors of the model. Even with the recognised limitations of the models, such calculations will continue to be of value as a tool with which to explore aspects of reaction mechanism which are not amenable to direct experimentation.

Acknowledgements

We thank the SERC for support of this research under grants GR/E53682 and GR/F49934.

References

1 B. Waszkowycz, I. H. Hillier, N. Gensmantel and D. W. Payling, *J. Chem. Soc., Perkin Trans. 2*, 1989, 1795.
2 B. Waszkowycz, I. H. Hillier, N. Gensmantel and D. W. Payling, *J. Chem. Soc., Perkin Trans. 2*, 1990, 1259.
3 B. Waszkowycz, I. H. Hillier, N. Gensmantel and D. W. Payling, *J. Chem. Soc., Perkin Trans. 2*, 1991, 225.
4 A. J. Slotboom, H. M. Verheij and G. H. de Haas, *New Comprehensive Biochemistry*, 1982, **4**, 354.
5 J. Chang, J. H. Musser and H. McGregor, *Biochem. Pharmacol.*, 1987, **36**, 2429.
6 H. M. Verheij, J. J. Volwerk, E. H. Jansen, W. C. Puyk, B. W. Dijkstra, J. Drenth and G. H. de Haas, *Biochem.*, 1980, **19**, 743.
7 (*a*) M. M. G. M. Thunnissen, A. B. Eiso, K. H. Kalk, J. Drenth, B. W. Dijkstra, O. P. Kuipers, R. Dijkman, G. H. de Haas and H. M. Verheij, *Nature*, 1990, **347**, 689; (*b*) D. L. Scott, S. P. White, Z. Otwinowski, W. Yuan, M. H. Gelb and P. B. Sigler, *Science*, 1990, **250**, 1541.
8 P. K. Weiner and P. A. Kollman, *J. Comput. Chem.*, 1981, **2**, 287.
9 M. F. Guest and J. Kendrick, GAMESS User Manual, CCP1/86/1, Daresbury Laboratory, UK, 1986.
10 (*a*) M. R. Pincus and H. A. Scheraga, *J. Am. Chem. Soc.*, 1979, **12**, 633; (*b*) J. M. Blaney, P. K. Weiner, A. Dearing, P. A. Kollman, E. C. Jorgensen, S. J. Oatley, J. M. Burridge and C. C. F. Blake, *J. Am.*

Chem. Soc., 1982, **104**, 6424; (*c*) G. Wipff, A. Dearing, P. K. Weiner, J. M. Blaney and P. A. Kollman, *J. Am. Chem. Soc.*, 1983, **105**, 997.
11 (*a*) R. Broer, P. T. van Duijnen and W. C. Nieuwpoort, *Chem. Phys. Lett.*, 1976, **42**, 525; (*b*) D. Demoulin and A. Pullman, *Theoret. Chim. Acta. (Berl.)*, 1978, **49**, 161; (*c*) S. Nakagawa, H. Umeyama and T. Kudo, *Chem. Pharm. Bull.*, 1980, **28**, 1342; (*d*) P. A. Kollman and D. M. Hayes, *J. Am. Chem. Soc.*, 1981, **103**, 2955; (*e*) R. Osman, H. Weinstein and S. Topiol, *Ann. NY Acad. Sci.*, 1981, **367**, 356.
12 (*a*) G. Bolis, M. Ragazzi, D. Salvaderi, D. R. Ferro and E. Clementi, *Gazz. Chim. Ital.*, 1978, **108**, 425; (*b*) G. Alagona, P. Desmeules, C. Ghio and P. A. Kollman, *J. Am. Chem. Soc.*, 1984, **106**, 3623; (*c*) S. J. Weiner, G. L. Seibel and P. A. Kollman, *Proc. Natl. Acad. Sci. USA*, 1986, **83**, 649; (*d*) D. Arad, R. Langridge and P. A. Kollman, *J. Am. Chem. Soc.*, 1990, **112**, 491.
13 (*a*) D. M. Hayes and P. A. Kollman, *J. Am. Chem. Soc.*, 1976, **98**, 7811; (*b*) L. C. Allen, *Ann. NY Acad. Sci.*, 1981, **367**, 383; (*c*) S. Nakagawa and H. Umeyama, *J. Theor. Biol.*, 1982, **96**, 473; (*d*) H. Umeyama, S. Hirono and S. Nakagawa, *Proc. Natl. Acad. Sci. USA*, 1984, **81**, 6266.
14 U. C. Singh and P. A. Kollman, *J. Comput. Chem.*, 1986, **7**, 718.
15 (*a*) A. Warshel and M. Levitt, *J. Mol. Biol.*, 1976, **103**, 227; (*b*) A. Warshel and R. M. Weiss, *J. Am. Chem. Soc.*, 1980, **102**, 6218; (*c*) J. Åqvist and A. Warshel, *Biochem.*, 1989, **28**, 4680; (*d*) M. J. Field, P. A. Bash and M. Karplus, *J. Comput. Chem.*, 1990, **11**, 700.
16 (*a*) P. Cieplak, P. Bash, U. C. Singh and P. A. Kollman, *J. Am. Chem. Soc.*, 1987, **109**, 6283; (*b*) P. A. Bash, U. C. Singh, F. K. Brown, R. Langridge and P. A. Kollman, *Science*, 1987, **235**, 574; (*c*) B. G. Rao and U. C. Singh, *J. Am. Chem. Soc.*, 1989, **111**, 3125.
17 R. W. Zwanzig, *J. Chem. Phys.*, 1954, **22**, 1420.
18 (*a*) U. C. Singh, F. K. Brown, P. A. Bash and P. A. Kollman, *J. Am. Chem. Soc.*, 1987, **109**, 1607; (*b*) P. A. Bash, U. C. Singh, R. Langridge and P. A. Kollman, *Science*, 1987, **236**, 564.
19 (*a*) M. H. Gelb, *J. Am. Chem. Soc.*, 1986, **108**, 3146; (*b*) W. Yuan, R. J. Berman and M. H. Gelb, *J. Am. Chem. Soc.*, 1987, **109**, 8071.
20 B. W. Dijkstra, K. H. Kalk, W. G. J. Hol and J. Drenth, *J. Mol. Biol.*, 1981, **147**, 97.
21 S. J. Weiner, P. A. Kollman, D. A. Case, U. C. Singh, C. Ghio, G. Alagona, S. Profeta and P. Weiner, *J. Am. Chem. Soc.*, 1984, **106**, 765.
22 S. J. Weiner, P. A. Kollman, D. T. Nguyen and D. A. Case, *J. Comput. Chem.*, 1986, **7**, 230.
23 U. C. Singh and P. A. Kollman, *J. Comput. Chem.*, 1984, **5**, 129.
24 P. B. Hitchcock, R. Mason, K. M. Thomas and G. G. Shipley, *Proc. Natl. Acad. Sci. USA*, 1974, **71**, 3036.
25 (*a*) A. A. Kossiakof and S. A. Spencer, *Biochem.*, 1981, **20**, 6462; (*b*) T. A. Steitz and R. G. Shulman, *Ann. Rev. Biophys. Bioeng.*, 1982, **11**, 419.
26 CADPAC. The Cambridge Analytical Derivatives Package, Issue 4.0, R. D. Amos and J. E. Rice, Cambridge, 1987.
27 B. L. Tembe and J. A. McCammon, *Comput. Chem.*, 1984, **8**, 281.
28 B. R. Brooks, R. E. Bruccoleri, B. D. Olafson, D. J. States, S. Swaminathan and M. Karplus, *J. Comput. Chem.*, 1983, **4**, 187.
29 A. Pluckthun, R. Rohlfs, F. F. Davidson and E. A. Dennis, *Biochemistry*, 1985, **24**, 4201.
30 G. H. de Haas, M. G. van Oort, R. Dijkman and R. Verger, *Biochem. Soc. Trans.*, 1989, **17**, 274.

Paper 1/02515E
Received 29*th May* 1991
Accepted 23*rd July* 1991